Determination of Molecular Subtypes of Diffuse Large B-Cell Lymphoma Using a Reverse Transcriptase Multiplex Ligation-Dependent Probe Amplification Classifier

Victor Bobée, Philippe Ruminy, Vinciane Marchand, Pierre-Julien Viailly, Ahmad Abdel Sater, Liana Veresezan, Fanny Drieux, Caroline C. Berard, Elodie Bohers, Sylvain Mareschal, et al.

Determination of Molecular Subtypes of Diffuse Large B-Cell Lymphoma Using a Reverse Transcriptase Multiplex Ligation-Dependent Probe Amplification Classifier

A CALYM Study

Victor Bobée,*† Philippe Ruminy,* Vinciane Marchand,* Pierre-Julien Viailly,* Ahmad Abdel Sater,*‡ Liana Veresezan,§ Fanny Drieux,*§ Caroline Bérard,‡ Elodie Bohers,* Sylvain Mareschal,* Sydney Dubois,* Jean-Philippe Jais,¶ Karen Leroy,‖ Martin Figeac,** Jean-Michel Picquenot,*§ Thierry Jo Molina,†† Gilles Salles,‡‡ Corinne Haioun,§§ Hervé Tilly,* and Fabrice Jardin*

From INSERM U1245 and LITIS EA 4108,‡ UNIROUEN, University of Normandie, Rouen; the Department of Biological Hematology,† Rouen University Hospital, Rouen; the Department of Pathology,§ Centre Henri Becquerel, Rouen; INSERM UMRS872,¶ AP-HP Necker Hospital, Paris; INSERM U955 Team 09,‖ AP-HP Henri Mondor Hospital, Creteil; the Functional Genomics Platform,** Center for Biology and Pathology, University of Lille, Lille Cedex; the Department of Pathology,†† Necker Hospital, AP-HP, Université Paris Descartes Sorbonne Cité, Paris; the Department of Hematology,‡‡ University Claude Bernard Lyon 1, Hospices Civils de Lyon, Pierre-Benite; and the Lymphoid Malignancies Unit,§§ Hospital Henri Mondor, Creteil, France*

Diffuse large B-cell lymphoma (DLBCL) is the most common non-Hodgkin lymphoma. It includes three major subtypes termed germinal center B-cell-like, activated B-cell-like, and primary mediastinal B-cell lymphoma. With the emergence of novel targeted therapies, accurate methods capable of interrogating this cell-of-origin classification should soon become essential in the clinics. To address this issue, we developed a novel gene expression profiling DLBCL classifier based on reverse transcriptase multiplex ligation-dependent probe amplification. This assay simultaneously evaluates the expression of 21 markers, to differentiate primary mediastinal B-cell lymphoma, activated B-cell-like, germinal center B-cell-like, and also Epstein-Barr viruse positive DLBCLs. It was trained using 70 paraffin-embedded biopsies and validated using >160 independent samples. Compared with a reference classification established from Affymetrix U133 þ 2 data, reverse transcriptase multiplex ligation-dependent probe amplification classified 85.0% samples into the expected subtype, comparing favorably with current diagnostic methods. This assay also proved to be highly efficient in detecting the MYD88 L265P mutation, even in archival paraffin-embedded tissues. This reliable, rapid, and cost-effective method uses common instruments and reagents and could thus easily be implemented into routine diagnosis workflows, to improve the management of these aggressive tumors.

Supported by grants from the French National Cancer Institute (INCA), the Ligue contre le Cancer (comité Seine Maritime), the Agir avec Becquerel Association, the Groupement des Entreprises Françaises dans la LUtte contre le Cancer (GEFLUC) Association, and the Consortium for the Acceleration of Innovation and its Transfer in the LYMphoma Field (CALYM).

V.B. and P.R. contributed equally to this work.

Disclosures: None declared.

Diffuse large B-cell lymphoma (DLBCL) is the most common non-Hodgkin lymphoma, accounting for nearly 40% of cases.[1] It is a heterogeneous disease that includes aggressive tumors of different mature B-cell origins. Two molecular subtypes have been identified by gene expression profiling (GEP).[2–4] The first, termed germinal center B-cell-like (GCB), is associated with a gene expression signature of normal germinal center B cells. Its prognosis is usually favorable, with a 5-year overall survival rate of almost 75%. The second, termed activated B-cell-like (ABC), develops from late GC B cells or plasmablasts. These lymphomas are more aggressive, and only 30% of patients can be cured using current therapy regimens.[5]

This ABC versus GCB cell-of-origin classification of DLBCLs is now recognized in the World Health Organization classification[6] and should soon have an important impact in the clinics. For example, because ABC DLBCL cell survival strongly depends on B-cell receptor signaling, specific inhibitors of the NF-κB pathway such as ibrutinib appear as promising alternatives to the current immune-chemotherapy–based regimens. Similarly, inhibitors of the enhancer of zeste homolog 2 (EZH2), B-cell lymphoma 2 (BCL2), and B-cell lymphoma 6 (BCL6) oncoproteins have shown encouraging results in GCB DLBCL. Accurate diagnostic methods capable of discriminating these subtypes are thus needed. Unfortunately, conventional histology is not informative; array-based GEP, considered the gold standard, is poorly adapted to daily diagnostic work; and the immunohistochemistry (IHC)-based algorithms used in most institutions experience a poor degree of reproducibility.[7,8] New dedicated GEP methods have thus emerged that show good sensitivity, specificity, and reproducibility, even when applied to formalin-fixed paraffin-embedded (FFPE) biopsies.[9,10]

An important limit of these methods is that they only inform on the GCB and ABC GEP signatures and do not recapitulate the true heterogeneity of these lymphomas. For example, a third important subtype of DLBCL, termed primary mediastinal B-cell lymphoma (PMBL), results from the transformation of thymic B cells. It usually arises in the mediastinum, in younger patients with a female predominance,[11,12] but recent evidence indicates that it can develop solely at nonmediastinal sites, making its diagnosis challenging.[13] In addition, the recognition of Epstein-Barr virus (EBV)-positive DLBCLs as a definitive entity[6] add further layers of complexity to the diagnosis of these aggressive tumors.

We have recently described a rapid and inexpensive reverse transcriptase multiplex ligation-dependent probe amplification (RT-MLPA) assay that allows for an accurate classification of GCB and ABC DLBCLs.[14] In the present study, we extended this assay to the identification of PMBL, the assessment of the EBV infection status, the detection of the ABC hallmark *MYD88* L265P mutation, and to the expression of multiple other prognostic factors and important therapeutic targets.

Materials and Methods

Patients

A total of 218 biopsy samples were used in this study (Supplemental Table S1). From the GHEDI (Deciphering the Genetic Heterogeneity of Diffuse large B-cell lymphoma in the rituximab era) study program, fresh/frozen biopsies of 150 DLBCL cases had previously been analyzed using U133 + 2 GEP arrays (Affymetrix, Santa Clara, CA). The HGU133 + 2.0 Affymetrix GeneChip microarray data set has been deposited in the National Center for Biotechnology Information's Gene Expression Omnibus (*https://www.ncbi.nlm.nih.gov/geo*; accession number GSE87371). Fifty-nine samples had been used in validation cohorts for the development of a first GCB-ABC predictor.[14] A total of 38 PMBL cases from the LNH07-3B trial ($n = 9$) and from the Center Henri Becquerel, Rouen, France ($n = 29$), were also included as well as 30 DLBCL cases from the Center Henri Becquerel. The diagnoses were established according to the World Health Organization 2008 criteria by expert pathologists.

RNA Extraction

For the 150 cases from the GHEDI study and the nine patients from the LNH07-3B trial, RNA samples were extracted from FFPE tissue using Siemens TPS and Versant reagents kit (Siemens Health Care Diagnostics, Erlangen, Germany). For PMBL from the Center Henri Becquerel, RNA was extracted from FFPE tissue for 22 patients using the Maxwell 16 system from Promega (Mannheim, Germany) and from frozen lymph node biopsies for seven patients. RNA from other DLBCLs was extracted from frozen lymph node biopsies when available ($n = 26$) and from FFPE tissue using the Maxwell 16 system ($n = 4$).

Immunohistochemistry and EBV Infection Status Evaluation

For the samples of the GHEDI cohort, the cell of origin classification was addressed by immunochemistry using the Hans algorithm, by evaluating CD10, BCL6, and melanoma-associated antigen (mutated) 1 (MUM1) expression.[15,16] Briefly, paraffin-embedded 3-μm-thick sections were subjected to antigen retrieval and antibody staining. The immunoperoxidase stains were performed on a Benchmark Ultra automated stainer (Roche Ventana, Tucson, AZ) using Ultraview Universal diaminobenzidine detection kits. In the absence of an internal positive control, immunostains were considered nonevaluable.

Chromogenic *in situ* hybridization for EBV-encoded small nuclear early region (EBER-ISH) was performed on FFPE tissue, sectioned at 4 μm, and placed on positively charged slides. Slides with specimens, as well as appropriate positive controls, were then placed in a 60°C oven for 1 hour and loaded onto the Ventana Benchmark XT for subsequent

Table 1 Sequences of RT-MLPA Probes and Competitors

5′ Probes	
EBER1L3	5′-GTGCCAGCAAGATCCAATCTAGAGTAGCCACCCGTCCCGGGTA-3′
CD5E3L	5′-GTGCCAGCAAGATCCAATCTAGACCACCACAACTCCAGAGCCCACAG-3′
NEK6E2F	5′-GTGCCAGCAAGATCCAATCTAGACCTGTGCATCCTCCTGACCCACAG-3′
IRF4E6F2	5′-GTGCCAGCAAGATCCAATCTAGACTGCCGAAGCCTTGGCGTTCTCAG-3′
MYDmF	5′-GTGCCAGCAAGATCCAATCTAGACAGGTGCCCATCAGAAGCGACC-3′
IGHME2F2	5′-GTGCCAGCAAGATCCAATCTAGAGCGTCCTCCATGTGTGGCCCCG-3′
CD30E3L2	5′-GTGCCAGCAAGATCCAATCTAGATTGTACAGCCTGCGTGACTTGTTCTCGAG-3′
CCND1E3F	5′-GTGCCAGCAAGATCCAATCTAGATACCTTCGTTGCCCTCTGTGCCACAG-3′
LMO2E5F	5′-GTGCCAGCAAGATCCAATCTAGACGGAAGCTCTGCCGGAGAGACTATCTCAG-3′
ITPKBE2F	5′-GTGCCAGCAAGATCCAATCTAGATACTACGGATCCAGCTGGCAGGACACGCAG-3′
FOXP1E10F3	5′-GTGCCAGCAAGATCCAATCTAGATCCCTTCCCCTTCAACCTCTTGCTCAAG-3′
MAML3E2F	5′-GTGCCAGCAAGATCCAATCTAGATACTCTTACGCTGCACTTCCATCCCACGGTCAG-3′
FCER2E7F3	5′-GTGCCAGCAAGATCCAATCTAGATATAGCTAAGGATGGAGTTGCAGGTGTCCAGCG-3′
TNFRSF13BF2	5′-GTGCCAGCAAGATCCAATCTAGATACTACTACTAGCGCACCTGTGCAGCCTTCTGCA-3′
MMEE10F	5′-GTGCCAGCAAGATCCAATCTAGATACTACTTACAAGGAGTCCAGAAATGCTTTCCGCAAG-3′
MYCE1F	5′-GTGCCAGCAAGATCCAATCTAGATACTACTACTTCGGGTAGTGGAAAACCAGCAGCCTC-3′
MALE3F	5′-GTGCCAGCAAGATCCAATCTAGATACTACTACTACTACGGTGGAGAGACTTCCTGGGTCACCTTG-3′
MYBL1E10F2	5′-GTGCCAGCAAGATCCAATCTAGATCCAGAATTTGCAGAGACTCTAGAACTTATTGAATCT-3′
CRBNE9F	5′-GTGCCAGCAAGATCCAATCTAGATACTACTACTGCCTTCTACAGAACACAGCTGGTTTCCTGG-3′
LIMD1E4F	5′-GTGCCAGCAAGATCCAATCTAGATACTACTACTACTTTCTTTGTGGACATCTGATCATGGACATG-3′
MS4A1E5F2	5′-GTGCCAGCAAGATCCAATCTAGATACTACTACTACTTTCTTCATGAGGGAATCTAAGACTTTGGGG-3′
3′ Probes	
EBER1R2	5′-Pho-CAAGTCCCGGGTGGTGAGGATATCCAACCCTTAGGGAACCC-3′
CD5E4R	5′-Pho-CTCCTCCCAGGCTGCAGCTGGTCCAACCCTTAGGGAACCC-3′
NEK6E3R	5′-Pho-AGGCATCCCAACACGCTGTCTTTTCCAACCCTTAGGGAACCC-3′
IRF4E7R	5′-Pho-ACTGCCGGCTGCACATCTGCCTGTATCCAACCCTTAGGGAACCC-3′
MYDmR	5′-Pho-GATCCCCATCAAGTACAAGGCAATGAAGAATCCAACCCTTAGGGAACCC-3′
IGHME3R	5′-Pho-ATCAAGACACAGCCATCCGGGTCTTCTACTATCCAACCCTTAGGGAACCC-3′
CD30E4R	5′-Pho-ACGACCTCGTGGAGAAGACGCCGTACTCCAACCCTTAGGGAACCC-3′
CCND1E4R	5′-Pho-ATGTGAAGTTCATTTCCAATCCGCCCTTACTTCCAACCCTTAGGGAACCC-3′
LMO2E6R	5′-Pho-GCTTTTTGGGCAAGACGGTCTCTGCTACTATCCAACCCTTAGGGAACCC-3′
ITPKBE3R	5′-Pho-GGAGTTTCAAGGCAGCTGCCAATGGCATACTATCCAACCCTTAGGGAACCC-3′
FOXP1E11R	5′-Pho-GCATGATTCCAACAGAACTGCAGCAGCTACTACTACTCCAACCCTTAGGGAACCC-3′
MAML3E3R	5′-Pho-GAGCAGCATCCAGTTGGACTTCCCCGAATACTTCCAACCCTTAGGGAACCC-3′
FCER2E8R	5′-Pho-GCTTTGTGTGCAACACGTGCCCTGAAAAGTTACTTCCAACCCTTAGGGAACCC-3′
TNFRSF13BE3R	5′-Pho-GGTCACTCAGCTGCCGCAAGGAGCTACTACTACTACTCCAACCCTTAGGGAACCC-3′
MMEE11R	5′-Pho-GCCCTTTATGGTACAACCTCAGAAACAGCATACTACTCCAACCCTTAGGGAACCC-3′
MYCE2R	5′-Pho-CCGCGACGATGCCCCTCAACGTTATACTACTACTACTATCCAACCCTTAGGGAACCC-3′
MALE4R	5′-Pho-GACGCAGCCTACCACTGCACCGTACTACTACTACTCCAACCCTTAGGGAACCC-3′
MYBL1E11R	5′-Pho-GATCCTGTAGCATGGAGTGACGTTACCAGTTTTTACTACTTCCAACCCTTAGGGAACCC-3′
CRBNE10R	5′-Pho-GTATGCCTGGACTGTTGCCCAGTGTAAGATTACTACTACTCCAACCCTTAGGGAACCC-3′
LIMD1E5R	5′-Pho-ATCCTGCAAGCCCTGGGGAAGTCCTACCTACTACTACTACTCCAACCCTTAGGGAACCC-3′
MS4A1E6R	5′-Pho-GCTGTCCAGATTATGAATGGGCTCTTCCACTACTACTACTATCCAACCCTTAGGGAACCC-3′
Competitors	
IRF4compF	5′-CTGCCGAAGCCTTGGCGTTCTCAG-3′
IgMCompF	5′-GCGTCCTCCATGTGTGGCCCCG-3′
LMO2compF	5′-CGGAAGCTCTGCCGGAGAGACTATCTCAG-3′
Foxp1compF	5′-CCCTTCCCCTTCAACCTCTTGCTCAAG-3′
MS4A1compF	5′-TTCTTCATGAGGGAATCTAAGACTTTGGGG-3′
NEK6compR	5′-TCCAACCCTTAGGGAACCC-3′

All sequences of the RT-MLPA probes and the oligonucleotides used as competitors are provided. The sequences of the primers used for PCR amplification are underlined.

RT-MLPA, reverse transcriptase multiplex ligation-dependent probe amplification.

deparaffinization, cell conditioning, enzymatic digestion (Protease 3; Ventana Medical Systems, Tucson, AZ), and *in situ* staining. The INFORM EBER Probe (Ref 800-2842; Ventana Medical Systems), used in combination with an anti−dinitrophenyl-biotin/streptavidin chromogen, was dispensed on the slides and incubated for 60 minutes. The iView Blue Detection Kit (Ventana Medical Systems) was used to produce the chromogenic reaction. Slides were

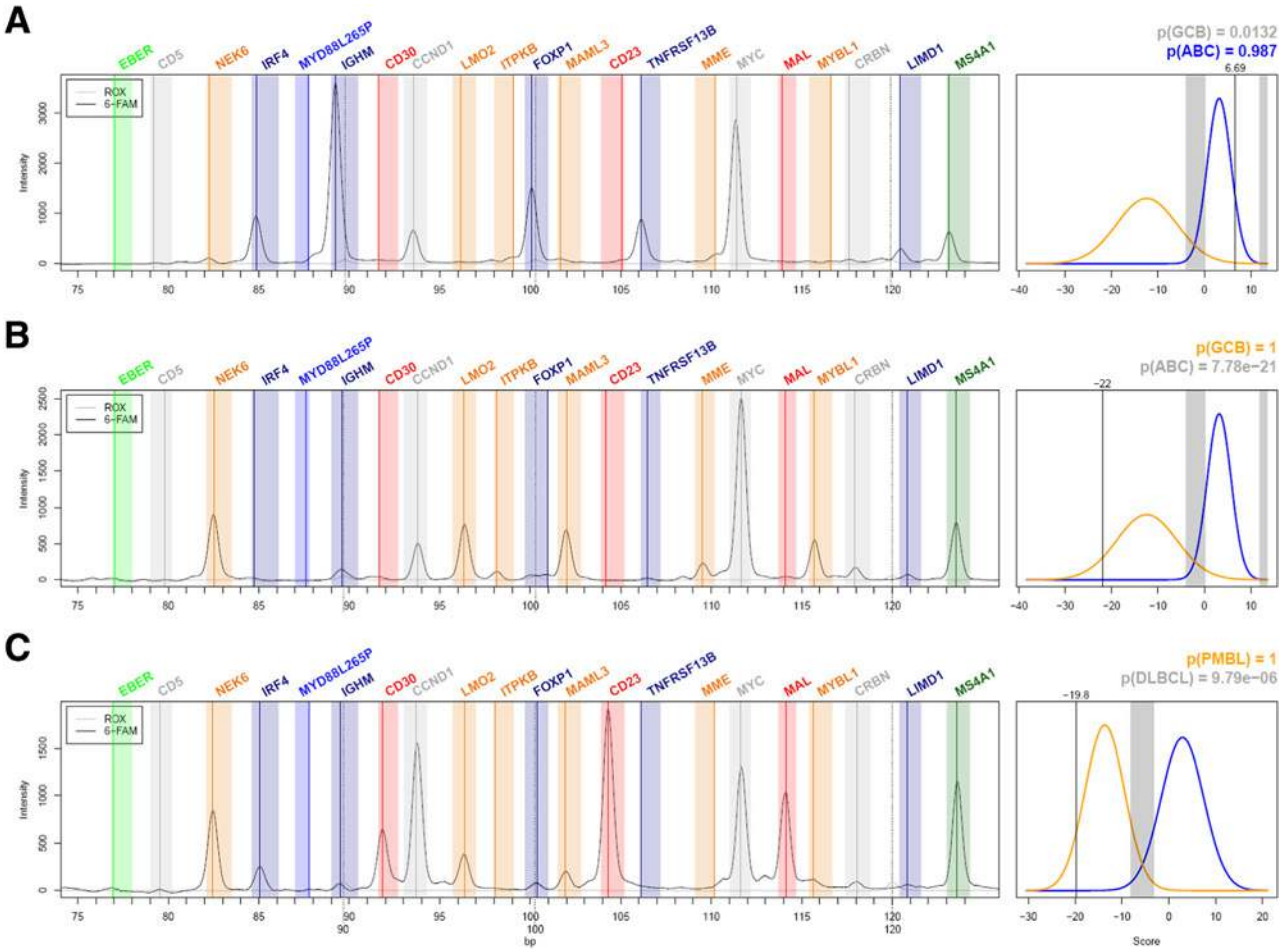

Figure 1 Representative reverse transcriptase multiplex ligation-dependent probe amplification (RT-MLPA) profiles. RT-MLPA profiles of three representative activated B-cell-like (ABC; **A**), germinal center B-cell-like (GCB; **B**), and primary mediastinal B-cell lymphoma (PMBL; **C**) samples. The **left panels** show the fragment-analysis profile (intensity of fluorescence as a function of the PCR fragment sizes), with intervals scanned for gene-related peaks highlighted in blue for ABC-related genes, orange for GCB-related genes, red for PMBL-related genes, green for Epstein-Barr virus (EBV) + diffuse large B-cell lymphoma (DLBCL)-specific *EBER* gene, dark green for *MS4A1* (encoding CD20) internal control, and gray for other genes. Size markers, used for the alignment of profiles and fragment size estimates (ROX channel), are shown with *dotted lines*, indicating their theoretical size. The **right panels** illustrate the cell of origin prediction retrieved by the Bayesian predictor.

counterstained using Ventana Medical Systems Red Stain II. After removal from the Benchmark XT, slides were manually dehydrated through graded ethanol solutions and xylene and then a nonaqueous mounting media was used as a coverslip.

Mutational Analysis

Samples from the GHEDI study have been analyzed in a previous study by a dedicated next-generation sequencing Lymphopanel, designed to identify mutations in 34 genes that are important for lymphomagenesis using an Ion Torrent Personal Genome Machine.[17] All *MYD88* L265P mutations were confirmed by Sanger sequencing.

RT-MLPA Probes and Reaction Mix

The sequences of the RT-MLPA probes are provided in Table 1 (Eurofins MWG Operon, Ebersberg, Germany). To avoid unwanted amplification of genomic DNA, all gene-specific pairs were designed across exon−exon boundaries. All comprised a gene-specific region complementary to the cDNA target and a primer for final PCR amplification. Two probes surrounding the *MYD88* L265P mutation were also designed, with the last nucleotide of the 5′ probe corresponding to the T>C substitution. Finally, two probes were designed to address the expression of the EBER1 transcript.

All 5′ probes have a GTGCCAGCAAGATCCAATCTAGA tail at their 5′ ends and all 3′ probes a TCCAACCCTTAGGGAACCC tail at their 3′ ends to allow for the final PCR amplification. Spacers of variable lengths were inserted between these primers and the target-specific sequences to allow for distinguishing the different PCR products according to their sizes. All 3′ probes were phosphorylated at their 5′ ends to allow the ligation reactions. Competitors identical to one of the probes but without the primers were added to the RT-MLPA probe mix to normalize the amplification signals.

The RT-MLPA probe mix was prepared from 10 μmol/L dilutions of probes and competitors in 10 mmol/L Tris, 1 mmol/L

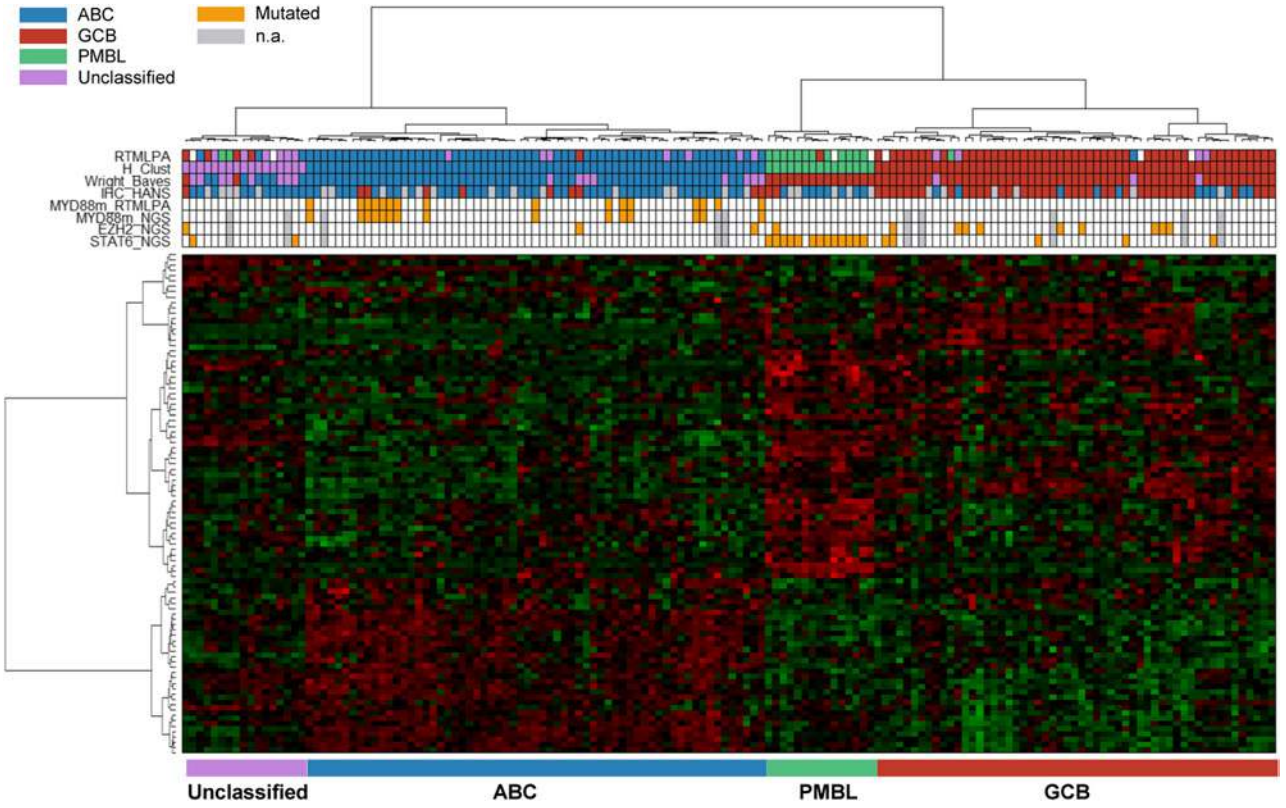

Figure 2 Cell of origin classification of the GHEDI (Deciphering the Genetic Heterogeneity of Diffuse large B-cell lymphoma in the rituximab era) series determined by unsupervised hierarchical clustering. Unsupervised hierarchical clustering of 150 patients from the GHEDI series, obtained from the Affymetrix gene expression data of 95 activated B-cell-like (ABC), germinal center B-cell-like (GCB), and primary mediastinal B-cell lymphoma (PMBL) discriminant genes. The results from the reverse transcriptase multiplex ligation-dependent probe amplification (RT-MLPA) classifier, hierarchical clustering (H-Clust), the Wright's predictor (Wright Bayes), and the Hans algorithm [immunohistochemistry (IHC) Hans] are provided. *MYD88* L265P mutational status determined by RT-MLPA (MYD88m_RTMLPA) and next-generation sequencing (MYD88_NGS) as well as *EZH2* (EZH2_NGS) and *STAT6* (STAT6_NGS) next-generation sequencing are indicated. n.a., not available.

EDTA buffer. The six competitors were first mixed with their corresponding probes at a 1:8 probe-to-competitor ratio for *IGHM*, 1:6 for *IRF4*, 1:4 for *FOXP1*, 1:3 for *NEK6*, and 1:2 for *LMO2* and *MS4A1* to normalize the levels of expression. A fixed volume (2 μL) of each probe ($n = 36$) or probe + competitor ($n = 6$) dilutions was next mixed to obtain a final volume of 84 μL. An equal volume of 20 mmol/L Tris, 2 mmol/L EDTA solution was then added to obtain a volume of 168 μL. The working solution was obtained by diluting 8.4 μL of this concentrated probe mix in 1 mL of 10 mmol/L Tris, 1 mmol/L EDTA solution.

RT-MLPA Assay and Data Processing

The protocol and data processing were as previously described,[14] using MLPA reagents from MRC-Holland (Amsterdam, The Netherlands). Briefly, 2 μL of total RNA from DLBCL biopsies, corresponding to 8 to 500 ng, was added to 3.75 μL of reverse transcription mix containing random hexamer primers. The samples were heated for 1 minute at 80°C to melt the secondary structure, incubated for 5 minutes at 37°C to allow the hybridization of the random primers, and cooled at 4°C. Next, 0.5 μL of Moloney murine leukemia virus reverse transcriptase was added, and the samples were incubated for 15 minutes at 37°C for cDNA synthesis, heated for 2 minutes at 98°C, and cooled at 4°C. Then, 3 μL of RT-MLPA probe mix was added (1.5 μL of SALSA-MLPA buffer and 1.5 μL of final dilution probe mix) before denaturation at 95°C for 2 minutes and hybridization at 60°C for 1 hour. Ligation of the annealed oligonucleotides was performed at 54°C for 15 minutes, adding 32 μL of ligation mix, and heated for 5 minutes at 98°C. Next, 2.5 μL of the ligation mixture was added to 7.5 μL of Salsa PCR master mix containing the labeled forward primer and the unlabeled reverse primer. PCR amplification involved 35 cycles of 94°C for 30 seconds, 58°C for 30 seconds, and 72°C for 30 seconds, followed by 72°C for 4 minutes. The resulting MLPA amplicons were analyzed by fragment analysis using an ABI 3130 XL capillary electrophoresis system (Applied Biosystems, Foster City, CA). For fragment analysis, 0.5 μL of PCR amplicon was mixed with 19 μL of Hi-di Formamide and 0.5 μL Genescan-400 HD ROX size standard (Applied Biosystems). The mixture was incubated for 3 minutes at 95°C and analyzed.

Statistical Analysis

Samples were classified using a linear predictor score and a Bayesian predictor, assuming that the distribution of the scores within the different groups was normal, allowing the estimation

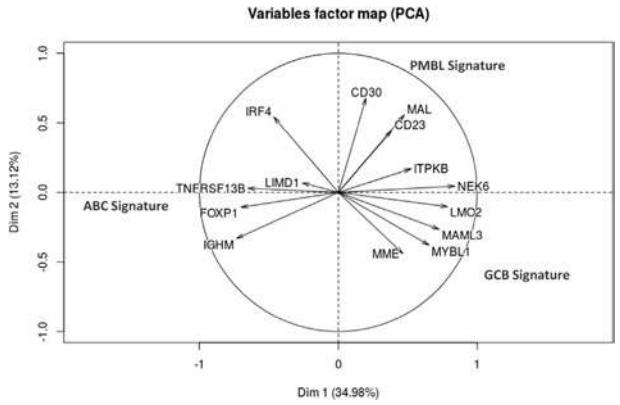

Figure 3 Principal component analysis (PCA) of the reverse transcriptase multiplex ligation-dependent probe amplification (RT-MLPA) gene expression results. The variable factor map was calculated based on the levels of expression of the 14 genes of the germinal center B-cell-like (GCB), activated B-cell-like (ABC), and primary mediastinal B-cell lymphoma (PMBL) signatures evaluated by RT-MLPA for the 143 analyzable samples of the GHEDI (Deciphering the Genetic Heterogeneity of Diffuse large B-cell lymphoma in the rituximab era) series. The relations between the genes of the ABC (*IGHM*, *FOXP1*, *TNFRSF13B*, *LIMD1*, and *IRF4*), GCB (*ITPKB*, *NEK6*, *LMO2*, *MAML3*, *MYBL1*, and *MME*), and PMBL (*CD30*, *MAL*, *CD23*, and *IRF4*) signatures are underlined.

of the probability for each case of belonging to one of the three DLBCL subtypes. Scaling factors were applied to balance the overweighting of the most highly expressed genes. To account for these differences in expression ranges, the *t* statistic that was used for the gene-specific coefficients was further divided by the mean expression of the corresponding genes in the training series. This interpretation of the results was made using dedicated homemade software (The RT-MLPA interface; *https://bioinfo.calym.org/RTMLPA*, registration required, last accessed June 27, 2017) that handles the entire analytic process, with a 90% confidence threshold to classify a sample. The Wilcoxon rank sum test was used to compare the expression of the different markers in the different subtypes.

Results

Gene Selection

Twenty-one genetic markers were included in the RT-MLPA assay. Eleven genes were selected from the literature to discriminate ABC from GCB cases (*ITPKB*, *LMO2*, *MAML3*, *MME*, *MYBL1*, *NEK6* for GCB; and *IRF4*, *FOXP1*, *IGHM*, *TNFRSF13B*, *LIMD1* for ABC) and three to identify PMBLs (*FCER2* encoding CD23, *TNFRSF8* encoding CD30, and *MAL*).[1,4,18–20] The EBER1 mRNA (EBV-encoded small nuclear early region) was included to assess the EBV infection status. Five additional markers were included as follows: *CCND1* overexpressed in mantle cell lymphoma, *CRBN* targeted by the immunomodulatory drugs lenalidomide and pomalidomide,[21] *MYC* and *CD5* whose expression is associated with a poor outcome, and *MS4A1* encoding the *CD20* receptor. Finally, two RT-MLPA probes were designed to examine the *MYD88* L265P hot-spot mutation status (Supplemental Figure S1). Representative RT-MLPA profiles of ABC, GCB, and PMBL cases are presented in Figure 1.

RT-MLPA Robustness

The RT-MLPA assay was applied to 150 RNA samples extracted from archival paraffin-embedded biopsies from the GHEDI study. Fourteen biopsies had been treated with an alcohol, formalin, acetic acid (AFA) fixative, 4 with a Bouin fixative, and 91 with formaldehyde. No information was available for the remaining cases obtained from different institutions. The median RNA concentration was 21 ng/μL (range, 4 to 94 ng/μL). Interpretable profiles were obtained for 143 of 150 cases (95.3%), including 13 of 14 AFA- and 3 of 4 Bouin-fixed samples (Supplemental Figures S2–S5), confirming the robustness of the RT-MLPA procedure despite the heterogeneity of the fixatives.

Class Prediction

The reference cell-of-origin classification was established by unsupervised hierarchical analysis (complete distance, Ward agglomeration) using HGU133 + 2.0 Affymetrix GeneChip arrays expression data obtained from frozen biopsies from the 150 cases of the GHEDI study (GEO, GSE87371). For this analysis, 56 GCB/ABC and 39 DLBCL/PMBL discriminant genes were selected from the literature (Supplemental Table S2).[3,4,9] Three clusters were delineated, allowing the identification of 63 ABC, 55 GCB, and 15 molecular PMBL (m-PMBL) cases (42%, 37%, and 10% of cases, respectively) (Figure 2). Seventeen samples (11%) could not be classified into any recognizable cluster and were considered unclassified. For validation, the same gene

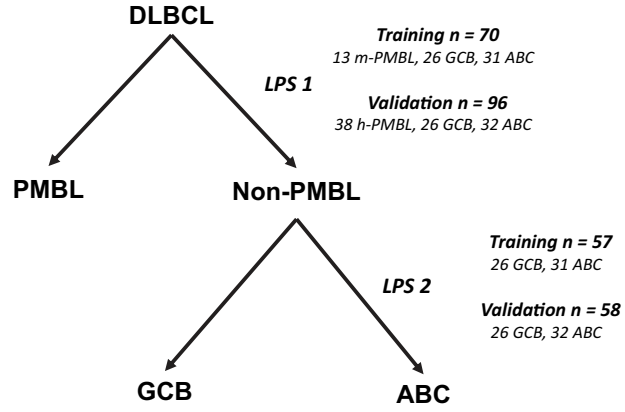

Figure 4 Principle of the reverse transcriptase multiplex ligation-dependent probe amplification (RT-MLPA) primary mediastinal B-cell lymphoma (PMBL)/activated B-cell-like (ABC)/germinal center B-cell-like (GCB) prediction. The RT-MLPA assay consists of two successive linear predictor scores (LPSs). The first LPS is designed to identify PMBL cases, whereas the second is designed to discriminate GCB from ABC cases. The number of samples that was included to design each LPS is indicated (training and validation cohorts). DLBCL, diffuse large B-cell lymphoma; h-PMBL, histologic primary mediastinal B-cell lymphoma; m-PMBL, molecular primary mediastinal B-cell lymphoma.

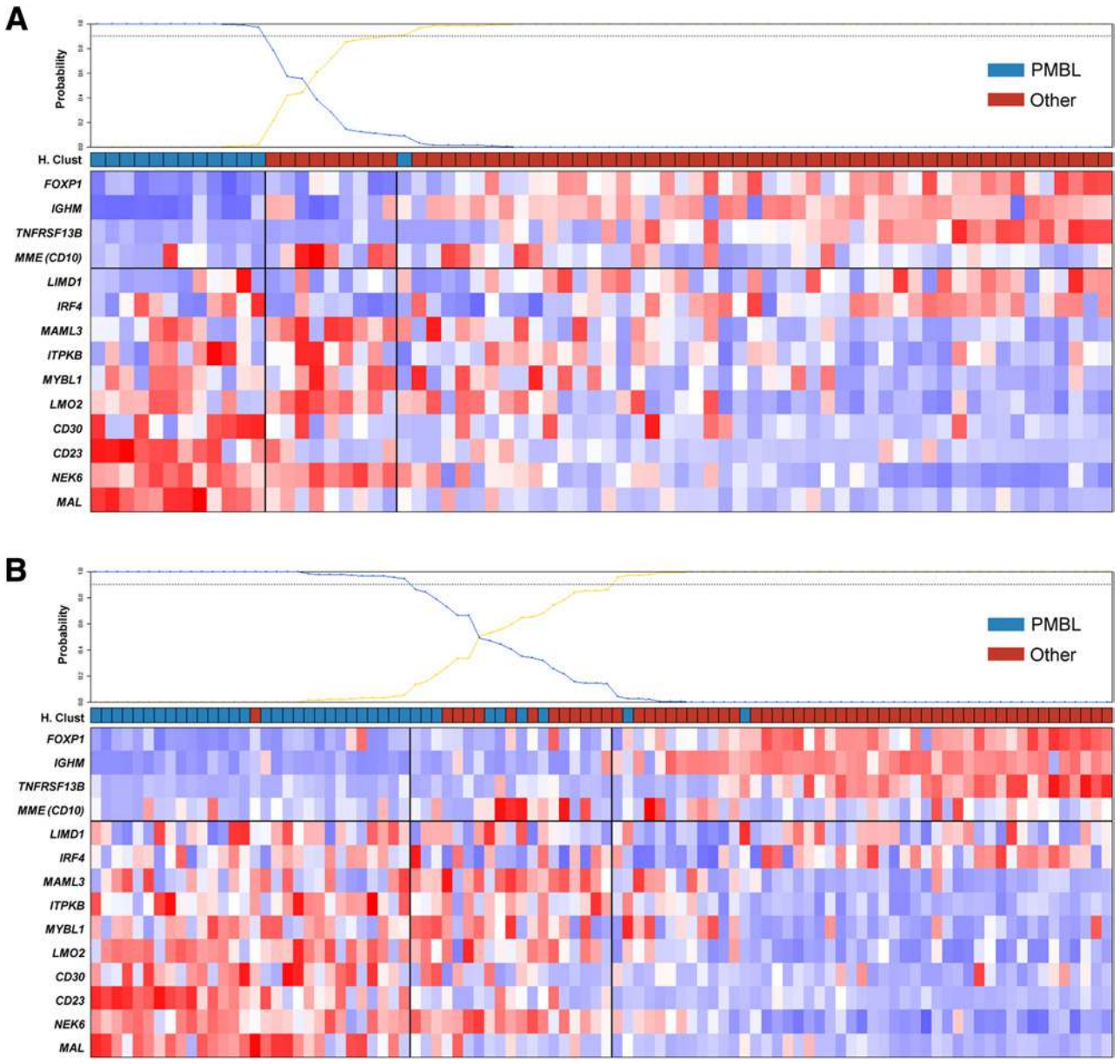

Figure 5 Reverse transcriptase multiplex ligation-dependent probe amplification (RT-MLPA) primary mediastinal B-cell lymphoma (PMBL) predictor training and validation. The expression of the 14 genes included in the PMBL predictor in the training (**A**) and validation (**B**) series is presented as heat maps (**bottom panels**), along with the expected classes computed with the Affymetrix-based unsupervised hierarchical clustering (**middle panels**) and the predicted probability of belonging to each of the groups (**top panels**). Samples (columns) are organized by ascending RT-MLPA scores, whereas genes (rows) are organized by their discriminating power (*t* statistics displayed on the right).

expression data set was analyzed using the Wright's algorithm as previously described.[3] Excluding the 15 PMBL cases, which, as expected, were classified within the GCB subtype, the two methods reached an agreement of 85.2%, confirming the validity of the hierarchical clustering analysis. In addition, next-generation sequencing (NGS) data indicated that 13 of the 15 PMBL cases identified by hierarchical clustering presented a mutation of the *STAT6* gene, particularly enriched in this lymphoma subtype.[22]

As shown in Figure 3, principal component analysis of the RT-MLPA data for the 143 analyzable cases of the GHEDI cohort delineated three subgroups of genes: *IGHM*, *FOXP1*, *TNFRSF13B*, and *LIMD1* (ABC DLBCLs signature); *CD30*, *MAL*, and *CD23* (PMBL signature); and *ITPKB*, *NEK6*, *LMO2*, *MAML3*, *MYBL1*, and *MME* (GCB DLBCLs signature). As expected, *IRF4*, which is expressed in most ABC DLBCLs and PMBLs, clearly distinguished those lymphoma from GCB cases.

To assign each case into one of these three subtypes, a linear predictor score method was applied to train two consecutive Bayesian predictors. The first was built to identify PMBL cases and the second to discriminate GCB

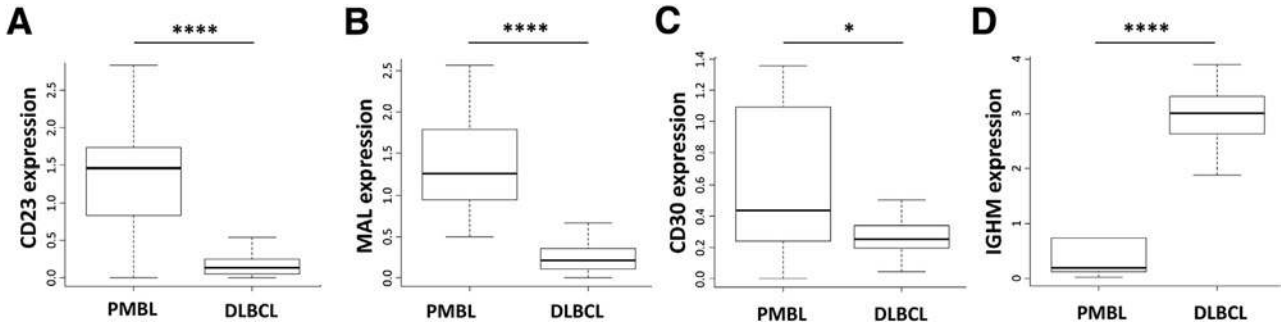

Figure 6 Differential expression of primary mediastinal B-cell lymphoma (PMBL) discriminant genes. Expression of *CD23* (**A**), *CD30* (**B**), *MAL* (**C**), and *IGHM* (**D**) markers in PMBL and germinal center B-cell-like (GCB)/activated B-cell-like (ABC) subgroups was determined using the reverse transcriptase multiplex ligation-dependent probe amplification (RT-MLPA) classifier in the GHEDI (Deciphering the Genetic Heterogeneity of Diffuse large B-cell lymphoma in the rituximab era) series. $*P < 0.05$, $****P < 0.0001$ by Wilcoxon test. DLBCL, diffuse large B-cell lymphoma.

from ABC cases (Figure 4). The first Bayesian predictor was trained using 70 GHEDI samples obtained by retaining all interpretable m-PMBL ($n = 13$) and by randomly selecting half of the GCB ($n = 26$) and half of the ABC ($n = 31$) cases (Figure 5). As expected, the three *CD23*, *CD30*, and *MAL* genes were significantly overexpressed in PMBL cases in this series (Figure 6, A−C). *IGHM* expression was also significantly lower in these lymphoma, which most often lack immunoglobulin expression (Figure 6D). Furthermore, other markers showed discriminant variations, including *LMO2* and *NEK6*, two GCB markers, and *TNFRSF13B* and *FOXP1*, two ABC markers.

In this training series, this first predictor correctly identified 12 of 13 m-PMBL cases (92.3%), and none of the 57 non-PMBL biopsies were incorrectly assigned to this subtype (Figure 5A). For validation, the same predictor was next applied to an independent series of 96 cases, which included all remaining GCB ($n = 26$) and ABC ($n = 32$) cases of the GHEDI cohort, complete with 38 histologic PMBLs. In this independent cohort, 29 histologic PMBLs were classified as PMBLs (76.3%), seven cases were considered unclassified (18.4%), and two cases were classified as non-PMBL (5.3%). Only one non-PMBL case of the GHEDI cohort (classified in the GCB subgroup by hierarchical clustering) was misclassified into this molecular subtype (Figure 5B).

A second Bayesian predictor was built to discriminate ABC from GCB cases. Again, a training series was obtained by randomly selecting half of the GCB ($n = 26$) and half of the ABC ($n = 31$) cases of the GHEDI cohort. In this series, 52 cases (91.2%) classified within the expected subtypes (28 ABC, 24 GCB) and five samples (3 ABC, 2 GCB) were considered unclassified (Figure 7A).

As expected, the expression of *ITPKB*, *LMO2*, *MAML3*, *NEK6*, and *MYBL1* were overexpressed in GCB cases (Figure 8, A−F), whereas *FOXP1*, *IRF4*, *LIMD1*, and *TNFRSF13B* was significantly associated with the ABC subtype (Figure 8, G−K). To validate this algorithm, a second independent cohort was analyzed, which comprised all remaining GCB ($n = 26$) and ABC ($n = 32$) cases. Here, 50 cases classified within the expected subtype (27 ABC and 23 GCB; 86.2%), 6 were considered unclassified (4 ABC and 2 GCB; 10.3%) and only 2 were misclassified (1 ABC and 1 GCB; 3.4%) (Figure 7B).

Overall, the RT-MLPA assay correctly assigned 85.0% of the ABC, GCB, and m-PMBL cases of the GHEDI cohort into the expected subtypes [55 of 63 ABC (87.3%); 46 of 55 GCB (83.6%); and 12 of 15 m-PMBL (80%)] (Table 2). Seven RT-MLPA profiles (4.7%) were considered uninterpretable, 11 cases (8.3%) were considered unclassified, and 4 cases (3.1%) were misclassified, with 2 GCB classified as ABC and PMBL, 1 ABC classified as GCB, and 1 m-PMBL classified as GCB. Interestingly, the only ABC case misclassified as GCB by RT-MLPA exhibited an *EZH2* Y644 mutation identified by NGS. The reason for this discrepancy was unknown, but a strong association between this mutation and the GCB GEP signature has been shown in previous studies.[17]

By comparison, the Hans IHC algorithm correctly assigned 78.8% of the ABC and GCB cases of the GHEDI cohort [53 of 63 ABC (84.1%) and 40 of 55 GCB (72.7%) cases] (Table 3). As expected, a majority of m-PMBL cases (10 of 14; 71.4%) were classified within the non-GCB subtype by IHC, due to a dominant CD10-negative, BCL6-positive, MUM1-positive immunophenotype. Finally, all 16 unclassified cases classified into the non-GCB subgroup using the Hans algorithm, and nine cases where considered uninterpretable because of a lack of informativity for at least one IHC marker.

MYD88 L265P Mutation Detection

We next verified the capacity of the RT-MLPA assay to correctly detect the *MYD88* L265P mutation. Ten positive control cases from the Center Henri Becquerel, where the mutation had been previously detected by Sanger sequencing, were tested. As shown in Figure 9A and Supplemental Figures S6−S8, all showed the expected signal. Sixteen *MYD88* L265P mutations were also detected in the GHEDI cohort. Fifteen had been previously identified by NGS with allele frequencies ranging from 19.8% to 82.1% (median, 46.2%), confirming the sensitivity of the

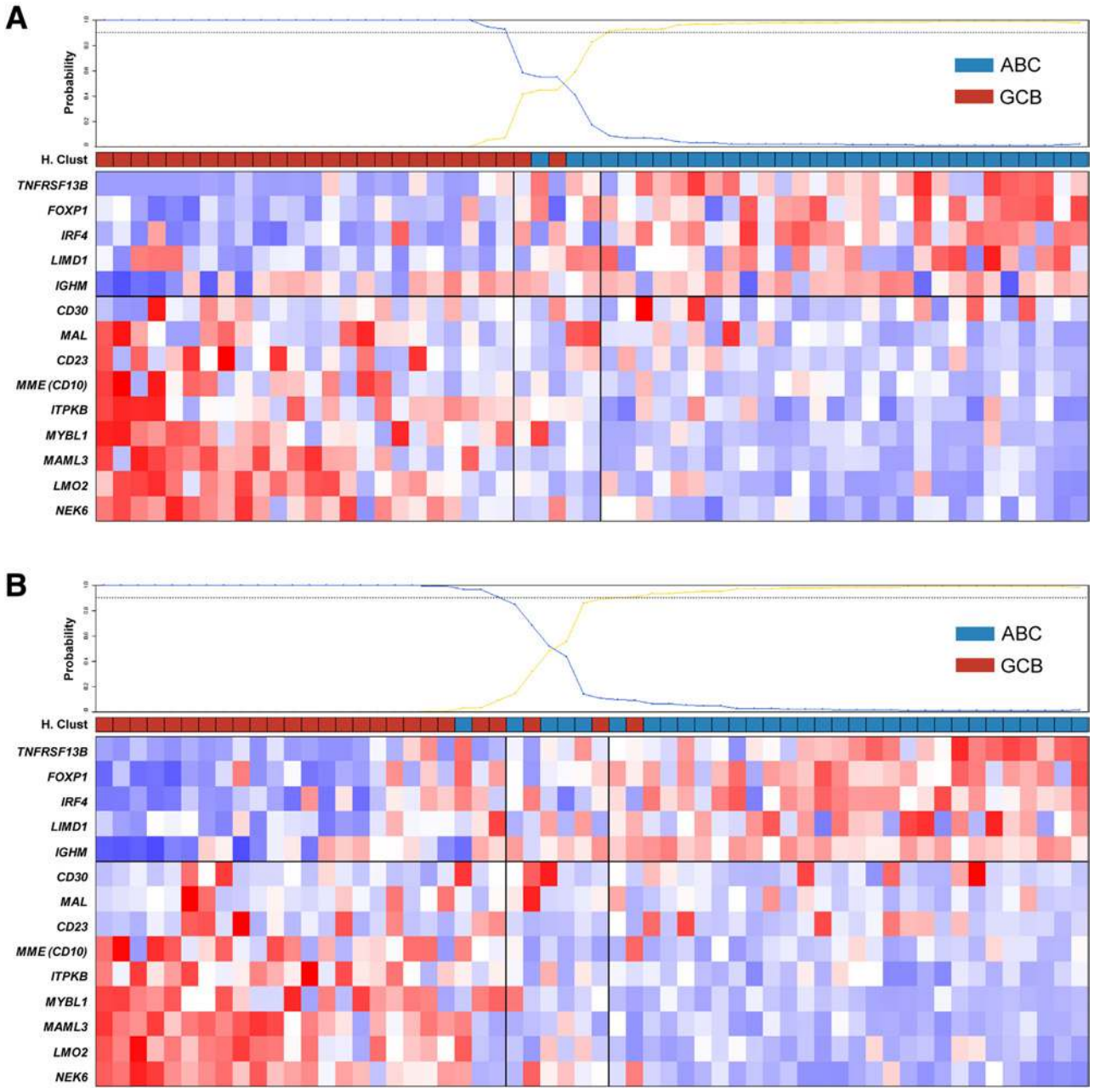

Figure 7 Reverse transcriptase multiplex ligation-dependent probe amplification (RT-MLPA) germinal center B-cell-like (GCB)/activated B-cell-like (ABC) predictor training and validation. The expression of the 14 genes included in the GCB/ABC predictor in the training (**A**) and validation (**B**) series is presented as heat maps (**bottom panels**), along with the expected classes computed with the Affymetrix-based unsupervised hierarchical clustering (**middle panels**) and the predicted probability of belonging to each of the groups (**top panels**). Samples (columns) are organized by ascending RT-MLPA scores, whereas genes (rows) are organized by their discriminating power (*t* statistics displayed on the right).

assay. The last mutated case of the GHEDI cohort was not analyzed by NGS because of a lack of available material. Importantly, no false-positive calls occurred in the 125 negative cases of the GHEDI cohort previously analyzed by NGS, confirming the specificity of the assay (positive predictive value and negative predictive value of 100%). Furthermore, as expected, all 26 mutated cases were classified within the ABC subtype using the Bayesian predictors, which does not take the presence of this marker into account for the classification.

EBV Infection Status Evaluation

We next verified the ability of the RT-MLPA assay to assess the EBV infection status. For the retrospective 10 EBV-positive and 10 EBV-negative control samples from the Center Henri Becquerel previously analyzed by ISH were tested. As shown in Figure 9B and Supplemental Figures S9–S11, all showed the expected *EBER* signal. Only one EBV-positive DLBCL case was identified in the GHEDI cohort, and it was considered unclassified by the RT-MLPA

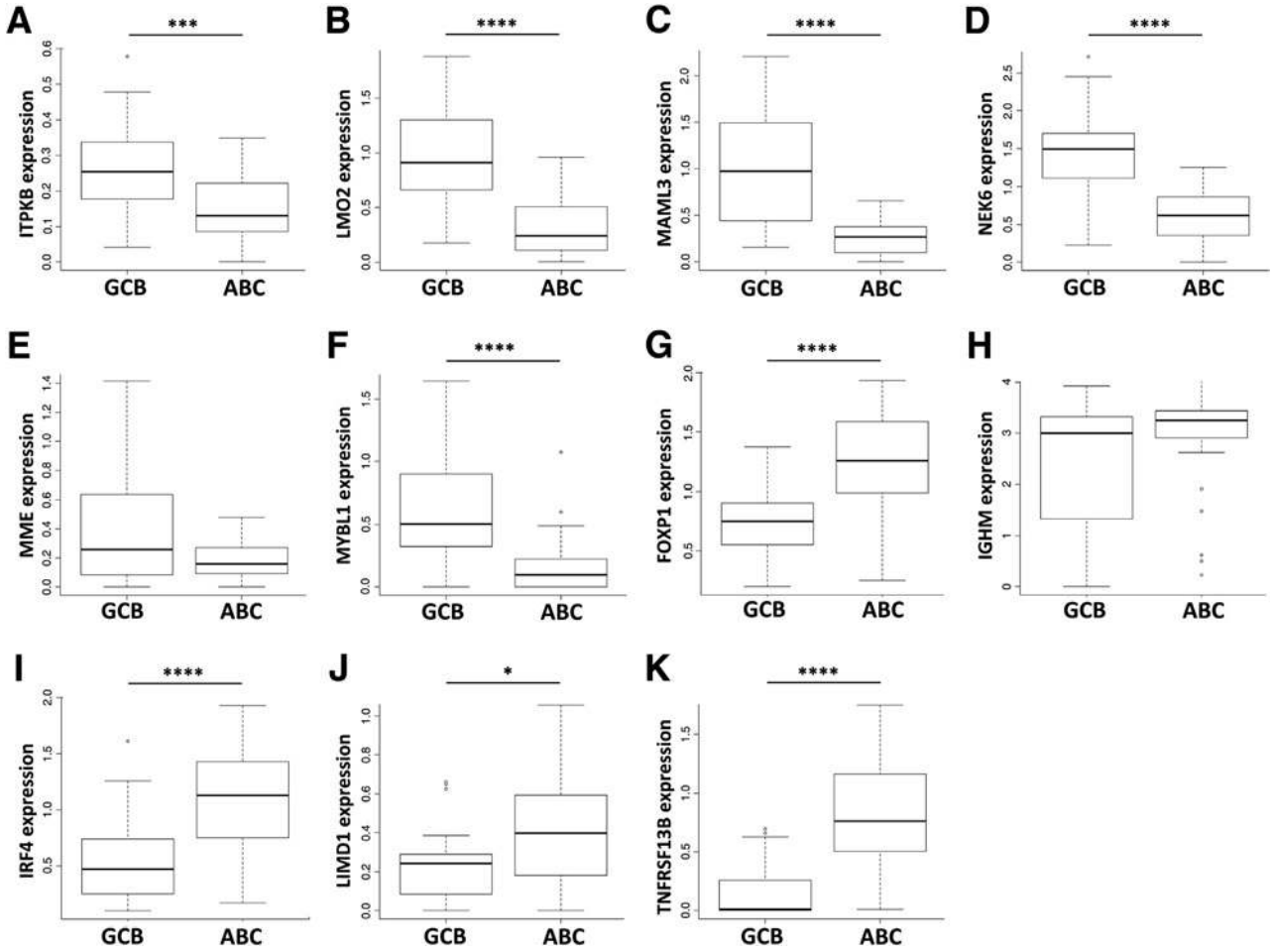

Figure 8 Differential expression of germinal center B-cell-like (GCB)/activated B-cell-like (ABC) marker genes. Expression of the markers included in the GCB/ABC predictors in the GCB (**A**–**F**) and ABC (**G**–**K**) subgroups was determined using the reverse transcriptase multiplex ligation-dependent probe amplification (RT-MLPA) classifier in the GHEDI (Deciphering the Genetic Heterogeneity of Diffuse large B-cell lymphoma in the rituximab era) series. *$P < 0.05$, ***$P < 0.001$, and ****$P < 0.0001$ by Wilcoxon test.

predictors, the hierarchical clustering approach, and the Wright's algorithm.

Discussion

In recent years, major advances have been made in the understanding of the heterogeneity of DLBCLs. According to the 2016 revision of the World Health Organization classification of lymphoid neoplasms, the different subtypes should now be identified at diagnosis. IHC algorithms are considered acceptable, but GEP-based methods are seen as promising alternatives. There is therefore an increasing need for accurate diagnostic tools that could be integrated into the diagnostic workflow.

The new RT-MLPA classifier we developed was trained using paraffin-embedded samples as available at most institutions. Interpretable gene expression profiles were obtained for 143 of 150 of the archival samples (95.3%) of the GHEDI cohort, demonstrating its robustness. Its capacity to provide reliable results even with Bouin- or AFA-treated biopsies, from which RNA extraction is generally considered highly challenging, confirms its resistance to RNA degradation. This advantage, which results from the very short RNA fragments required for the correct hybridization of the RT-MLPA probes, could prove particularly useful in daily practice. The

Table 2 Comparison of RT-MLPA and Affymetrix GEP Results

	RT-MLPA				
Affymetrix	GCB	ABC	PMBL	Unclassified	Failure
GCB	46	1	1	4	3
ABC	1	55	0	7	0
PMBL	1	0	12	0	2
Unclassified	5	3	2	5	2

Cell of origin classification of the GHEDI (Deciphering the Genetic Heterogeneity of Diffuse large B-cell lymphoma in the rituximab era) series determined by RT-MLPA compared with unsupervised hierarchical clustering from Affymetrix data. All data are expressed as *n*.

ABC, activated B-cell-like; GCB, germinal center B-cell-like; GEP, gene expression profiling; PMBL, primary mediastinal B-cell lymphoma; RT-MLPA, reverse transcriptase multiplex ligation-dependent probe amplification.

Table 3 Comparison of Immunochemistry and Affymetrix GEP Results

	Hans IHC		
Affymetrix	GCB	Non-GCB	n.i.
GCB	40	10	5
ABC	8	53	2
PMBL	4	10	1
Unclassified	0	16	1

Cell of origin classification of the GHEDI (Deciphering the Genetic Heterogeneity of Diffuse large B-cell lymphoma in the rituximab era) series determined by IHC (Hans algorithm) compared with unsupervised hierarchical clustering from Affymetrix data. All data are expressed as *n*.

ABC, activated B-cell-like; GCB, germinal center B-cell-like; GEP, gene expression profiling; IHC, immunohistochemistry; n.i., not interpretable; PMBL, primary mediastinal B-cell lymphoma.

concordance of the RT-MLPA results with the gold standard Affymetrix classification compares favorably with other diagnostic methods such as immunochemistry. More specifically, and as could be verified on the GHEDI cohort, gene expression-based assay can directly identify ABC cases through the expression of specific markers and do not attribute the samples by default into a non-GCB category when no GCB markers are detected. Its capacity to interrogate the *MYD88* L265P mutation and the EBV infection status as well as other important markers such as MS4A1 (CD20) or CD30, which are not systematically addressed by IHC, could also be particularly useful for therapeutic decision. It also appears as an interesting tool to discriminate PMBL from other DLBCLs, which could soon benefit from targeted therapies.

The diagnosis of PMBL is usually evoked when patients present with mediastinal involvement. However, the diagnosis of these tumors is often challenging, and recent studies have suggested that not all cases show this typical presentation.[13] When applied to these tumors, the Hans IHC algorithm usually returns a non-GCB classification because of a predominant *CD10*$^{-}$ *BCL6*$^{+}$ MUM1 immunophenotype. By contrast, the RT-MLPA assay allows a systematic evaluation of three important PMBL markers, *CD30*, *CD23*, and *MAL*, as well as *MME* (which encodes CD10, usually negative in these pathologic processes), *IGHM* (usually negative), and *IRF4* (usually positive). It could thus be particularly useful to identify these cases with atypical clinical presentations. It can also differentiate PMBLs from other DLBCLs that may, by chance, originate in the mediastinal region. This probably occurred for case CHB_1570, initially diagnosed as a PMBL because of its mediastinal localization, but which clearly showed an ABC gene expression profile.

Our assay also correctly identified all control EBV-positive cases and one additional case in the GHEDI cohort. Furthermore, applied to the 23 last consecutive cases who presented in our institution, RT-MLPA and EBV-ISH showed a 100% agreement, with 2 positive and 21 negative cases identified (data not shown). EBV-positive DLBCL of the elderly was introduced in the 2008 World Health Organization classification of lymphoid neoplasms as a provisional entity restricted to patients older than 50 years and is in general associated with a poor prognosis.[23] However, a recent study comparing older and younger patients reported no significant clinical differences,[24] leading to the extension of this subtype to all ages in the 2016 revision of the classification. Its prevalence is estimated between 5% and 15% of all DLBCL cases,[23] but because EBV testing is not systematically performed at diagnosis, many cases are probably managed as EBV-negative DLBCLs. Still, new

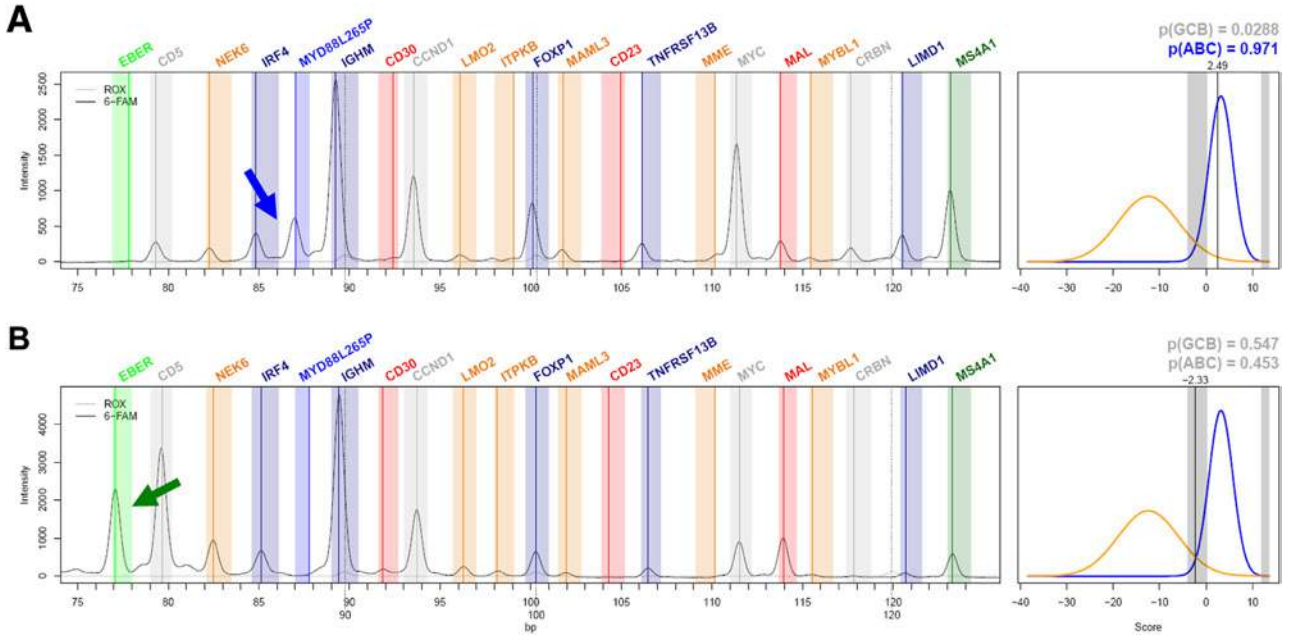

Figure 9 Additional reverse transcriptase multiplex ligation-dependent probe amplification (RT-MLPA) profiles. RT-MLPA for two representative samples: the *MYD88* L265P mutation is indicated with a **blue arrow** (**A**); Epstein-Barr virus-encoded small nuclear early region (EBER) expression, indicating Epstein-Barr virus (EBV) infection, with a **green arrow** (**B**). ABC, activated B-cell-like; GCB, germinal center B-cell-like.

promising therapeutic approaches are currently under evaluation for these diseases, including antiviral therapy in combination with EBV lytic phase induction,[25] EBV specific cytotoxic T lymphocytes[26] or chimeric antigen receptor T cells. The RT-MLPA assay could thus allow a more systematic identification of those patients.

Among the other therapeutic markers included in the assay, *CD30* is a therapeutic target.[27–29] Likewise, cereblon is a direct target of lenalidomide and pomalidomide, two drugs currently under clinical evaluation for these tumors.[21] The systematic evaluation of these markers by RT-MLPA could thus be particularly useful in prospective clinical trials testing these new therapies. In addition, the RT-MLPA approach proved to be particularly efficient in detecting the *MYD88* L265P mutation, one of the most common genetic abnormalities in ABC DLBCLs, and may be predictive of ibrutinib sensitivity.[30,31]

Conclusions

RT-MLPA appears as an efficient, rapid, and cost-effective alternative to the current methods used in the clinic to establish the cell of origin classification of DLBCLs. In contrast to other technologic approaches such as RNAseq or Nanostring technologies, its implementation requires only common laboratory equipment, that is, a thermal cycler and a capillary genetic analyzer, and does not necessitate the acquisition of any specialized platform. By allowing the identification of the three major DLBCL subtypes and a simultaneous evaluation of multiple prognostic and theranostic markers and therapeutic targets, RT-MLPA could contribute to a more efficient management of these aggressive tumors in both clinical trials and daily practice.

Acknowledgments

We thank Dr. Marie Hélène Delfau and Dr. Camille Laurent for the careful reading of the manuscript and their helpful comments.

V.B., P.R., and V.M. designed and performed research, analyzed and interpreted data, and wrote the manuscript; E.B. and S.D. performed research and participated in the interpretation of the data; P.-J.V., A.A.S., C.B., S.M., J.-P.J., and M.F. analyzed the data and developed the class prediction algorithm; L.V., F.D., T.J.M., and J.-M.P. performed histologic reviews; K.L. and T.J.M. coordinated sample collection for the LYSA group; G.S., C.H., H.T., and F.J. coordinated the study and supervised analysis.

Supplemental Data

Supplemental material for this article can be found at *https://doi.org/10.1016/j.jmoldx.2017.07.007*.

References

1. Swerdlow SH, Campo E, Harris NL: Mature B-cell neoplasms: diffuse large B-cell lymphoma, not otherwise specified. WHO Classification of Tumours of Haematopoietic and Lymphoid Tissues, ed 4. Edited by Swerdlow SH, Campo E, Harris NL, Jaffe ES, Pileri SA, Stein H, Thiele J, Vardiman JW. Lyon, France: International Agency for Research on Cancer, 2008. pp. 233–237
2. Alizadeh AA, Eisen MB, Davis RE, Ma C, Lossos IS, Rosenwald A, Boldrick JC, Sabet H, Tran T, Yu X, Powell JI, Yang L, Marti GE, Moore T, Hudson J Jr, Lu L, Lewis DB, Tibshirani R, Sherlock G, Chan WC, Greiner TC, Weisenburger DD, Armitage JO, Warnke R, Levy R, Wilson W, Grever MR, Byrd JC, Botstein D, Brown PO, Staudt LM: Distinct types of diffuse large B-cell lymphoma identified by gene expression profiling. Nature 2000, 403:503–511
3. Wright G, Tan B, Rosenwald A, Hurt EH, Wiestner A, Staudt LM: A gene expression-based method to diagnose clinically distinct subgroups of diffuse large B cell lymphoma. Proc Natl Acad Sci U S A 2003, 100:9991–9996
4. Rosenwald A, Wright G, Leroy K, Yu X, Gaulard P, Gascoyne RD, et al: Molecular diagnosis of primary mediastinal B cell lymphoma identifies a clinically favorable subgroup of diffuse large B cell lymphoma related to Hodgkin lymphoma. J Exp Med 2003, 198:851–862
5. Lenz G, Staudt LM: Aggressive lymphomas. N Engl J Med 2010, 362: 1417–1429
6. Swerdlow SH, Campo E, Pileri SA, Harris NL, Stein H, Siebert R, Advani R, Ghielmini M, Salles GA, Zelenetz AD, Jaffe ES: The 2016 revision of the World Health Organization classification of lymphoid neoplasms. Blood 2016, 127:2375–2390
7. Salles G, de Jong D, Xie W, Rosenwald A, Chhanabhai M, Gaulard P, Klapper W, Calaminici M, Sander B, Thorns C, Campo E, Molina T, Lee A, Pfreundschuh M, Horning S, Lister A, Sehn LH, Raemaekers J, Hagenbeek A, Gascoyne RD, Weller E: Prognostic significance of immunohistochemical biomarkers in diffuse large B-cell lymphoma: a study from the Lunenburg Lymphoma Biomarker Consortium. Blood 2011, 117:7070–7078
8. Gutiérrez-García G, Cardesa-Salzmann T, Climent F, González-Barca E, Mercadal S, Mate JL, Sancho JM, Arenillas L, Serrano S, Escoda L, Martínez S, Valera A, Martínez A, Jares P, Pinyol M, García-Herrera A, Martínez-Trillos A, Giné E, Villamor N, Campo E, Colomo L, López-Guillermo A; Grup per l'Estudi dels Limfomes de Catalunya I Balears (GELCAB): Gene-expression profiling and not immunophenotypic algorithms predicts prognosis in patients with diffuse large B-cell lymphoma treated with immunochemotherapy. Blood 2011, 117:4836–4843
9. Scott DW, Wright GW, Williams PM, Lih C-J, Walsh W, Jaffe ES, Rosenwald A, Campo E, Chan WC, Connors JM, Smeland EB, Mottok A, Braziel RM, Ott G, Delabie J, Tubbs RR, Cook JR, Weisenburger DD, Greiner TC, Glinsmann-Gibson BJ, Fu K, Staudt LM, Gascoyne RD, Rimsza LM: Determining cell-of-origin subtypes of diffuse large B-cell lymphoma using gene expression in formalin-fixed paraffin-embedded tissue. Blood 2014, 123:1214–1217
10. Masqué-Soler N, Szczepanowski M, Kohler CW, Spang R, Klapper W: Molecular classification of mature aggressive B-cell lymphoma using digital multiplexed gene expression on formalin-fixed paraffin-embedded biopsy specimens. Blood 2013, 122:1985–1986
11. Savage KJ, Al-Rajhi N, Voss N, Paltiel C, Klasa R, Gascoyne RD, Connors JM: Favorable outcome of primary mediastinal large B-cell lymphoma in a single institution: the British Columbia experience. Ann Oncol 2006, 17:123–130
12. Cazals-Hatem D, Lepage E, Brice P, Ferrant A, d'Agay MF, Baumelou E, Brière J, Blanc M, Gaulard P, Biron P, Schlaifer D, Diebold J, Audouin J: Primary mediastinal large B-cell lymphoma. A clinicopathologic study of 141 cases compared with 916 non-mediastinal large B-cell lymphomas, a GELA ("Groupe d'Etude des Lymphomes de l'Adulte") study. Am J Surg Pathol 1996, 20: 877–888

13. Yuan J, Wright G, Rosenwald A, Steidl C, Gascoyne RD, Connors JM, Mottok A, Weisenburger DD, Greiner TC, Fu K, Smith L, Rimsza LM, Jaffe ES, Campo E, Martinez A, Delabie J, Braziel RM, Cook JR, Ott G, Vose JM, Staudt LM, Chan WC; Lymphoma Leukemia Molecular Profiling Project (LLMPP): Identification of primary mediastinal large B-cell lymphoma at nonmediastinal sites by gene expression profiling. Am J Surg Pathol 2015, 39:1322−1330
14. Mareschal S, Ruminy P, Bagacean C, Marchand V, Cornic M, Jais J-P, Figeac M, Picquenot J-M, Molina TJ, Fest T, Salles G, Haioun C, Leroy K, Tilly H, Jardin F: Accurate classification of germinal center B-cell-like/activated B-cell-like diffuse large B-cell lymphoma using a simple and rapid reverse transcriptase-multiplex ligation-dependent probe amplification assay: a CALYM study. J Mol Diagn 2015, 17: 273−283
15. Hans CP, Weisenburger DD, Greiner TC, Gascoyne RD, Delabie J, Ott G, Müller-Hermelink HK, Campo E, Braziel RM, Jaffe ES, Pan Z, Farinha P, Smith LM, Falini B, Banham AH, Rosenwald A, Staudt LM, Connors JM, Armitage JO, Chan WC: Confirmation of the molecular classification of diffuse large B-cell lymphoma by immunohistochemistry using a tissue microarray. Blood 2004, 103:275−282
16. Molina TJ, Canioni D, Copie-Bergman C, Recher C, Brière J, Haioun C, Berger F, Fermé C, Copin M-C, Casasnovas O, Thieblemont C, Petrella T, Leroy K, Salles G, Fabiani B, Morschauser F, Mounier N, Coiffier B, Jardin F, Gaulard P, Jais J-P, Tilly H: Young patients with non-germinal center B-cell-like diffuse large B-cell lymphoma benefit from intensified chemotherapy with ACVBP plus rituximab compared with CHOP plus rituximab: analysis of data from the Groupe d'Etudes des Lymphomes de l'Adulte/lymphoma study association phase III trial LNH 03-2B. J Clin Oncol 2014, 32:3996−4003
17. Dubois S, Viailly P-J, Mareschal S, Bohers E, Bertrand P, Ruminy P, Maingonnat C, Jais J-P, Peyrouze P, Figeac M, Molina TJ, Desmots F, Fest T, Haioun C, Lamy T, Copie-Bergman C, Brière J, Petrella T, Canioni D, Fabiani B, Coiffier B, Delarue R, Peyrade F, Bosly A, André M, Ketterer N, Salles G, Tilly H, Leroy K, Jardin F: Next-generation sequencing in diffuse large B-cell lymphoma highlights molecular divergence and therapeutic opportunities: a LYSA study. Clin Cancer Res 2016, 22:2919−2928
18. Pileri SA, Zinzani PL, Gaidano G, Falini B, Gaulard P, Zucca E, Sabattini E, Ascani S, Rossi M, Cavalli F; International Extranodal Lymphoma Study Group: Pathobiology of primary mediastinal B-cell lymphoma. Leuk Lymphoma 2003, 44 Suppl 3:S21−S26
19. Copie-Bergman C, Gaulard P, Maouche-Chrétien L, Brière J, Haioun C, Alonso MA, Roméo PH, Leroy K: The MAL gene is expressed in primary mediastinal large B-cell lymphoma. Blood 1999, 94:3567−3575
20. Higgins JP, Warnke RA: CD30 expression is common in mediastinal large B-cell lymphoma. Am J Clin Pathol 1999, 112:241−247
21. Zhang L-H, Kosek J, Wang M, Heise C, Schafer PH, Chopra R: Lenalidomide efficacy in activated B-cell-like subtype diffuse large B-cell lymphoma is dependent upon IRF4 and cereblon expression. Br J Haematol 2013, 160:487−502
22. Ritz O, Guiter C, Castellano F, Dorsch K, Melzner J, Jais J-P, Dubois G, Gaulard P, Möller P, Leroy K: Recurrent mutations of the STAT6 DNA binding domain in primary mediastinal B-cell lymphoma. Blood 2009, 114:1236−1242
23. Castillo JJ, Beltran BE, Miranda RN, Young KH, Chavez JC, Sotomayor EM: EBV-positive diffuse large B-cell lymphoma of the elderly: 2016 update on diagnosis, risk-stratification, and management. Am J Hematol 2016, 91:529−537
24. Monabati A, Vahedi A, Safaei A, Noori S, Mokhtari M, Vahedi L, Zamani M: Epstein-Barr virus-positive diffuse large B-cell lymphoma: is it different between over and under 50 years of age? Asian Pac J Cancer Prev 2016, 17:2285−2289
25. Ghosh SK, Perrine SP, Williams RM, Faller DV: Histone deacetylase inhibitors are potent inducers of gene expression in latent EBV and sensitize lymphoma cells to nucleoside antiviral agents. Blood 2012, 119:1008−1017
26. Wilkie GM, Taylor C, Jones MM, Burns DM, Turner M, Kilpatrick D, Amlot PL, Crawford DH, Haque T: Establishment and characterization of a bank of cytotoxic T lymphocytes for immunotherapy of epstein-barr virus-associated diseases. J Immunother 2004, 27:309−316
27. Hu S, Xu-Monette ZY, Balasubramanyam A, Manyam GC, Visco C, Tzankov A, Liu W, Miranda RN, Zhang L, Montes-Moreno S, Dybkær K, Chiu A, Orazi A, Zu Y, Bhagat G, Richards KL, Hsi ED, Choi WWL, Han van Krieken J, Huang Q, Huh J, Ai W, Ponzoni M, Ferreri AJ, Zhao X, Winter JN, Zhang M, Li L, Møller MB, Piris MA, Li Y, Go RS, Wu L, Medeiros LJ, Young KH: CD30 expression defines a novel subgroup of diffuse large B-cell lymphoma with favorable prognosis and distinct gene expression signature: a report from the International DLBCL Rituximab-CHOP Consortium Program Study. Blood 2013, 121:2715−2724
28. Ok CY, Li L, Xu-Monette ZY, Visco C, Tzankov A, Manyam GC, Montes-Moreno S, Dybkaer K, Dybaer K, Chiu A, Orazi A, Zu Y, Bhagat G, Chen J, Richards KL, Hsi ED, Choi WWL, van Krieken JH, Huh J, Ai W, Ponzoni M, Ferreri AJ, Farnen JP, Møller MB, Bueso-Ramos CE, Miranda RN, Winter JN, Piris MA, Medeiros LJ, Young KH: Prevalence and clinical implications of epstein-barr virus infection in de novo diffuse large B-cell lymphoma in Western countries. Clin Cancer Res 2014, 20:2338−2349
29. Delacruz W, Setlik R, Hassantoufighi A, Daya S, Cooper S, Selby D, Brown A: Novel Brentuximab vedotin combination therapies show promising activity in highly refractory CD30+ non-Hodgkin lymphoma: a case series and review of the literature. Case Rep Oncol Med 2016, 2016:2596423
30. Ngo VN, Young RM, Schmitz R, Jhavar S, Xiao W, Lim K-H, Kohlhammer H, Xu W, Yang Y, Zhao H, Shaffer AL, Romesser P, Wright G, Powell J, Rosenwald A, Muller-Hermelink HK, Ott G, Gascoyne RD, Connors JM, Rimsza LM, Campo E, Jaffe ES, Delabie J, Smeland EB, Fisher RI, Braziel RM, Tubbs RR, Cook JR, Weisenburger DD, Chan WC, Staudt LM: Oncogenically active MYD88 mutations in human lymphoma. Nature 2011, 470:115−119
31. Wilson WH, Young RM, Schmitz R, Yang Y, Pittaluga S, Wright G, Lih C-J, Williams PM, Shaffer AL, Gerecitano J, de Vos S, Goy A, Kenkre VP, Barr PM, Blum KA, Shustov A, Advani R, Fowler NH, Vose JM, Elstrom RL, Habermann TM, Barrientos JC, McGreivy J, Fardis M, Chang BY, Clow F, Munneke B, Moussa D, Beaupre DM, Staudt LM: Targeting B cell receptor signaling with ibrutinib in diffuse large B cell lymphoma. Nat Med 2015, 21:922−926